

# Ultrabroadband sound control of 3D spaces using plasmacoustic metalayers

Stanislav Sergeev<sup>1</sup>

Acoustic Group - Signal Processing Laboratory LTS2, EPFL, Lausanne, Switzerland

Mark Donaldson<sup>2</sup>

Sonexos SA, Lausanne, Switzerland

Hervé Lissek<sup>3</sup>

Acoustic Group - Signal Processing Laboratory LTS2, EPFL, Lausanne, Switzerland

## ABSTRACT

*Controlling sound in three-dimensional spaces is a complex task, challenged by the intricacies of acoustic modal structures, the variety of noise sources, and the propagation of waves. This research analyzes the influence of local impedance control on the global sound field within a parallelepipedal volume characterized by high reverberation. The employed electroacoustic transducer is based on a corona discharge mechanism and utilizes the Plasmacoustic Metalayer concept. The sound field is regulated directly by the interaction between the air particles and the ionized air produced in the discharge area. The inertia-free Plasmacoustic Metalayer contributes to an increased control bandwidth. Experimental tests conducted with several actively controlled transducers distributed throughout the volume demonstrate the dampening of multiple modes. This leads to a more consistent frequency response and a broadband reduction in sound pressure levels across the entire space, demonstrated here up to 700 Hz. Numerical simulations suggest that such a system can also be potentially efficient in a more realistic space such as a vehicle cabin.*

## 1. INTRODUCTION

Active noise reduction techniques have seen significant advancements in recent decades, driven by extensive scientific and engineering focus. In some instances, these advancements have culminated in developing mature products. Notably, noise can be substantially diminished across a wide frequency range in relatively controlled acoustic environments as in the case of the ear canal. [1, 2]. In waveguides, such as exhaust and ventilation ducts, active noise cancellation techniques are effective in reducing sound pressure levels [3]. Yet, achieving noise reduction in generic three-dimensional spaces with active techniques remains a challenging task. Currently, the most effective strategies in these environments largely depend on using passive noise reduction materials, including porous and resonant absorbers [4]. Due to the significant mass and volume needed for effective broadband and low-frequency noise reduction, passive materials

---

<sup>1</sup>stanislav.sergeev@epfl.ch

<sup>2</sup>mark.donaldson@sonexos.com

<sup>3</sup>herve.lissek@epfl.ch

are not always the best fit for certain applications. For instance, incorporating acoustic materials into a vehicle cabin can adversely affect its acceleration and power consumption. In contrast, active noise reduction, including active noise cancellation and active sound absorption, offers the possibility of enhancing acoustic performance with minimal impact on vehicle performance.

Active noise cancellation (ANC) systems in passenger vehicles aim to minimize cabin noise using multi-channel adaptive feedforward techniques, notably the filtered-x LMS algorithm. These systems incorporate an array of reference and error sensors, usually microphones accelerometers, that are distributed throughout the cabin, alongside multiple loudspeakers embedded within the door panels and trunk. Effective noise reduction, particularly for engine-generated noise up to 200 Hz, is achievable when reference signals, like engine speed, are measured directly [5, 6]. Challenges arise in mitigating noise from other sources, including road movement and wind, due to difficulties in identifying suitable reference signals. Consequently, additional sensors, typically accelerometers, strategically placed in the vehicle's chassis, drivetrain, and engine compartment become necessary [7, 8]. The system's effectiveness in reducing road and wind noise is generally confined to the 400-500 Hz range. Enhancements in performance are possible through the integration of remote microphone sensing and passenger head tracking [9, 10], although these improvements introduce greater system complexity and increased costs, hindering practical implementation. Furthermore, the spatial areas within which noise control is effective remain relatively small, limited to a portion of the noise wavelength. Therefore, there is a pressing need for further research and development to explore alternative strategies that can enhance ANC performance and extend the noise reduction zone within the cabin.

Active sound absorption can change the acoustic properties of the space by treating a small part of the surfaces with active transducers [11, 12]. A transducer is typically configured to deliver an acoustic impedance that corresponds to perfect or partial sound absorption. In previous work, a principle of plasmacoustic metalayer was introduced [13]. Controlling a thin layer of ionized air with an alternating electrical field makes it possible to interact with the sound field. Perfect sound absorption under normal sound incidence was achieved over more than 1 kHz due to the absence of moving mass in such a transducer as demonstrated in an impedance tube. The plasmacoustic metalayer has a very compact form factor and can be designed in different sizes and shapes without compromising its acoustic properties.

In this work, we investigate the potential of controlling plasmacoustic metalayers to reduce noise via active sound absorption in a three-dimensional context. A model rectangular volume of 2 m<sup>3</sup> with relatively high reverberation is considered as the environment for the numerical and experimental assessment of the active concept. Transducers with a plasmacoustic metalayer (plasmacoustic transducers) are controlled to achieve sound-absorbing condition. Noise reduction as well as response equalization inside the tested volume is evaluated. Finally, we bridge our work with the realistic application by modelling a car cabin with more damped interior acoustics and numerically investigate the potential noise reduction if such a plasmacoustic sound absorption (PASA) system is implemented.

## **2. PRESENTATION OF THE TEST ENVIRONMENT**

A rectangular volume is built for the evaluation of the PASA system (Figure 1). The frame is made from aluminium profiles and the walls are composed of 20 mm thick MDF panels. The internal dimensions of the cabin are L=1210 mm × W=1150 mm × H=1460 mm. A compact loudspeaker (ELAC 301.2) is used as the noise source inside the volume. It is located in the corner with the membrane center set off by 10 cm from each plane of the corner. The sound pressure level spectra are recorded with microphones at different locations inside the volume. Since there are no acoustic materials on the surface of the test volume, the acoustics is relatively reverberant and presents a modal behavior. For this study, four plasmacoustic transducers with 130 × 130 mm<sup>2</sup>

active surface each are mounted at the corners of the same wall. The number of transducers was determined in preliminary numerical simulations, as the minimum to obtain a noticeable acoustic effect, for example, 3 dB broadband noise reduction.

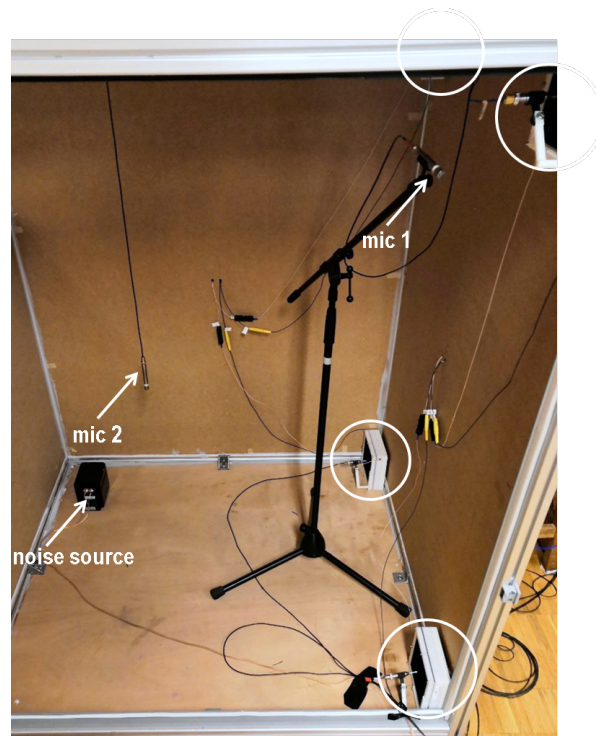


Figure 1: The rectangular volume for the evaluation of the PASA system. The noise source is placed in the corner, measurement microphones are fixed at different locations. Locations of plasmacoustic transducers are shown by the white circles.

A COMSOL Multiphysics finite element model is designed to calculate the system's potential performance before the measurements. The modelled acoustic domain is the the same rectangular volume as designed for the experiment. The sound source is modelled as a point monopole source with constant power output located at one corner and set off by 10 cm from each wall. This is a reasonable and simple approximation because the size of the loudspeaker used in the experiment and its membrane are smaller than the wavelength for frequencies up to approximately 1 kHz. The geometry of the plasmacoustic transducers and their locations in the model correspond to the experimental setup.

The acoustic boundary condition for the walls of the modelled volume should be set to make the passive response representative with regard to the experimental data. For this purpose, frequency responses at several locations in the volume are recorded experimentally. Then, the walls' "boundary impedance" is adjusted to match the modelled response to the measured one. Figure 2 compares two responses measured with the microphone located 20 cm from the volume corner (microphone 1 in Figure 1). As can be seen, the overall modelled response follows the measured curve. The peak-to-dip ranges are similar except for the first several modes. This happens because of the increased sound transmission in experimental volume due to the relatively low mass of the walls and the low-frequency response of the loudspeaker source. Nevertheless, the shape of the modes is well modelled up to 400 Hz. At higher frequencies, the slight deviations in positions of the plasmacoustic transducers, measurement points, and approximation of the noise source do not allow for precise reconstruction of the modal shapes. Only peak-to-dip dynamics and modal density are of importance to model accurately at high frequencies as they represent the amount of acoustic losses in the volume and will influence

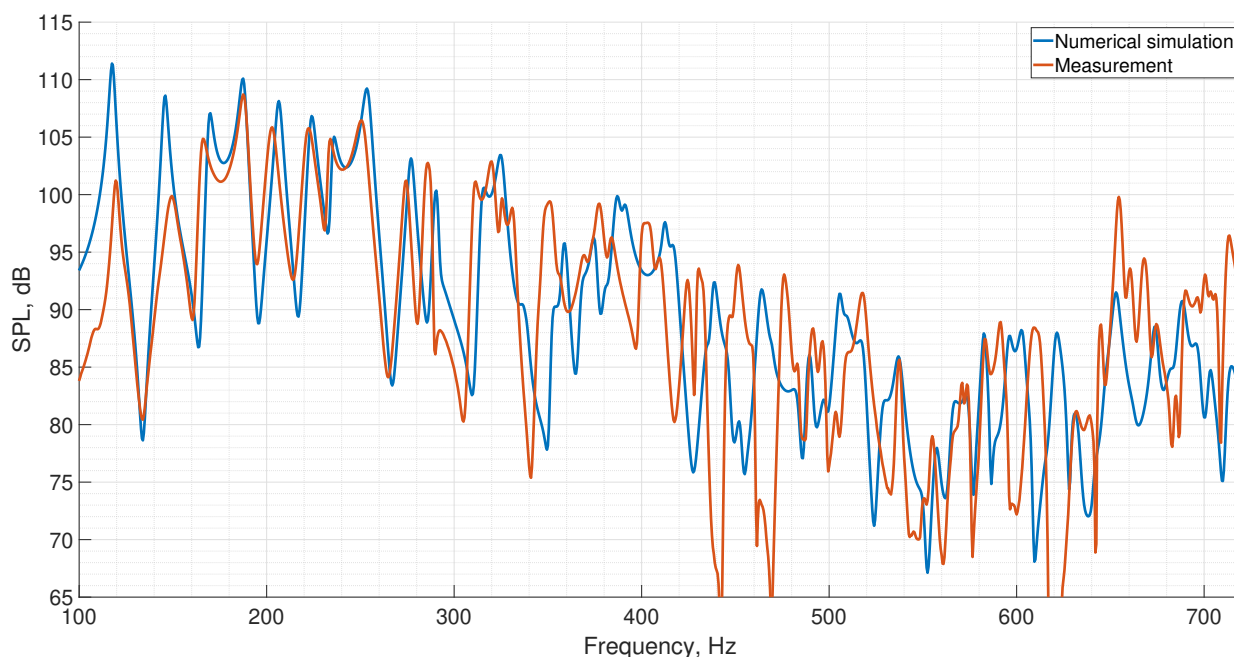


Figure 2: Sound pressure level spectra measured experimentally and calculated in the numerical model at the microphone position located 20 cm from the volume corner. A sound absorption coefficient of 3.5% is assigned to all volume's walls as the boundary condition.

the relative performance of the active sound absorption system. Therefore, a constant effective absorption coefficient boundary can be used as the boundary condition to simulate a simple 3D space like this rectangular volume with wooden walls. An absorption coefficient of 3.5% is assigned to all the walls in the numerical model. It should provide a representative environment for simulating the control of the PASA system with further experimental validation.

### 3. PLASMACOUSTIC TRANSDUCER AND CONTROL PRINCIPLE

The plasmacoustic transducer prototype to be used in the experimental assessment is shown in Figure 3. The emitter electrode is made of a thin nichrome wire, which is arranged in a back-and-forth pattern of parallel wire lengths equally spaced and fixed inside the rigid plastic frame. The collector electrode is fabricated from a perforated metallic plate. This electrode has a sufficiently large open area ratio to be acoustically transparent. The active area of the metalayer established between the electrodes  $130 \times 130 \text{ mm}^2$ , the separation between the corona and collector electrodes is 5 mm. A stable corona discharge is produced if the voltage difference in the 5.5-9 kV range is applied to the electrodes. The ionized particles interact with the surrounding neutral air by transmitting the mechanical force and depositing a portion of heat losses from the discharge zone. If the alternating voltage is added to the constant one, the ionized part of the air changes its velocity according to the electrical input signal that finally generates an acoustic signal. Thus, the plasmacoustic metalayer presents a combination of so-called "force" and "heat" acoustic sources, as described in [13].

The transducer is backed with a rigid plastic wall. It also features an ozone filter at the front face to prevent the space from any possible contamination. The sound transmission coefficient of the filter was measured to be almost 100% at low frequencies and to gradually drop to 96% at 1 kHz. Thus, its influence on acoustic wave propagation is considered negligible and is not accounted for in the controller design or numerical simulations. The control microphone picks the signal in the center of the active area.

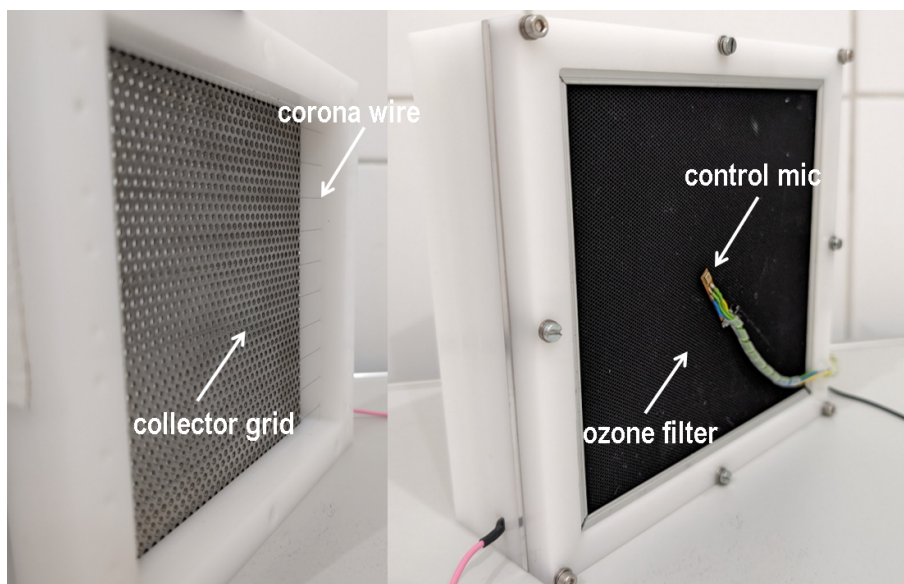


Figure 3: Left - electrode arrangement to establish the plasmacoustic metalayer. Right - fully-assembled plasmacoustic transducer from the back with rigid enclosure at the back and ozone filter. A control microphone is installed on the front of the transducer.

For the numerical simulations, the plasmacoustic metalayer is represented by an air layer of  $130 \times 130 \text{ mm}^2$  area and thickness of 5 mm. This volume acts as a source of uniform mechanical force and heat power with densities, as was proposed in [13]. However, the geometry of the whole transducer is simplified. The electrode arrangement and ozone filter are not included in the simulation due to their low acoustic impact. The transducer's volume is terminated by the boundary with impedance  $Z_L = 23 \cdot 10^3 \text{ Pa} \cdot \text{s} \cdot \text{m}^{-1}$  at a distance of 25 mm from the active layer. This reflects the average value of the real part of the termination impedance which was measured in the impedance tube with the actual prototype. The pressure virtually sensed at a distance of 10 mm in front of the metalayer is used as input for the modelled control loop. The active control strategy consists in achieving a predefined acoustic impedance at the front of the plasmacoustic metalayer. With the prescribed impedance condition, various reflective or absorbing conditions with a controlled phase can be realized [13]. The controller processes a target transfer function which is based on the analytical model of the plasmacoustic metalayer. It links the sensed pressure to the voltage required to achieve a target impedance at the microphone position. The analytical model requires knowledge of the force and heat source magnitudes. To calibrate the strengths of these sources, the voltage-current characteristics of the actual transducer prototype should be measured. The procedure is described in [14]. Additionally, the PASA system described herein incorporates features covered by the granted US patent US11790881B2 [15] and various pending patent applications worldwide.

#### 4. SIMULATION RESULTS WITH PASA SYSTEM

The active control system with four plasmacoustic transducers is implemented in the frequency domain simulation in Comsol Multiphysics. Here, the control transfer function is set so as to target the characteristic impedance of the air  $Z_0 = \rho c$ , where  $\rho$  is the air density and  $c$  is the speed of sound in the air. This impedance condition leads to a perfect sound absorption condition under normal wave incidence. Figure 4 demonstrates the simulated performance of the PASA system comparing passive and active frequency responses calculated at a single point (corresponds to the position of microphone 1 in Figure 1). If the system is passive, the plasmacoustic transducers almost do not provide any sound absorption since the enclosures are



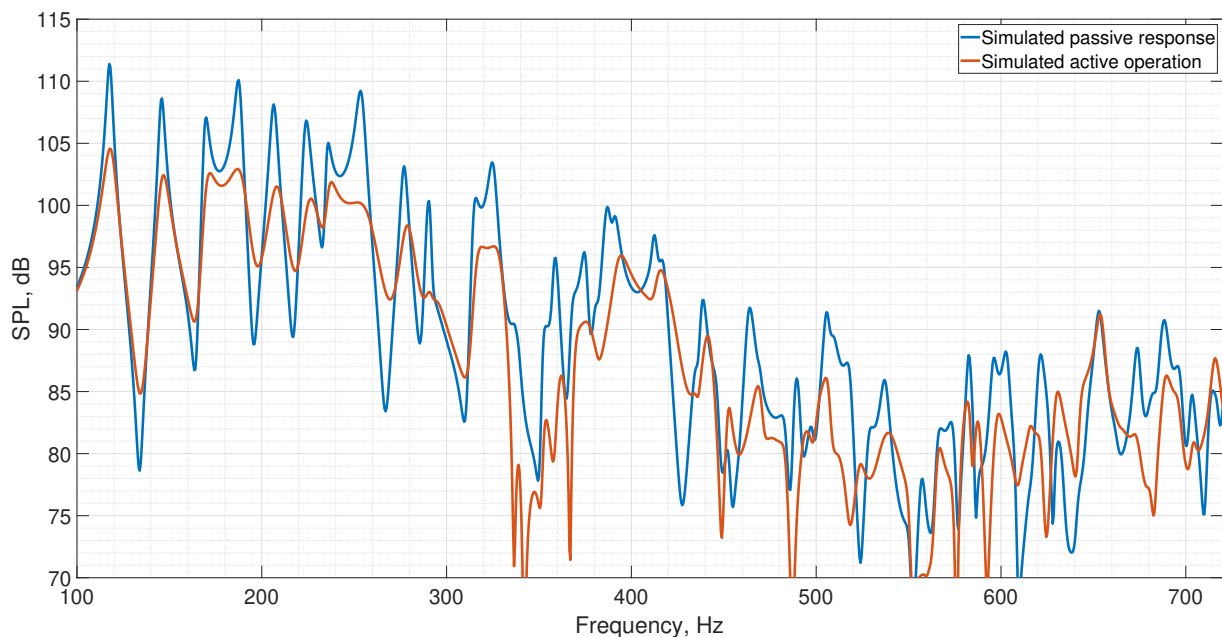


Figure 4: Simulated frequency response at a single point of the test volume. Blue - PASA system turned off; red - system targets  $Z_0$  impedance.

built from rigid plastic. The acoustic modes inside the volume are prominent across the simulated frequency range. However, when the control is set to actively target  $Z_0$ , the response becomes significantly more damped. Each low frequency mode reduces its peak-to-dip dynamics and some higher frequency modes become indistinguishable. Consequently, this additional damping leads to the equalization of the frequency response and reduction of the sound pressure levels over the considered frequency range. The average noise reduction equals 3.3 dB in the frequency range up to 400 Hz and 3.0 dB up to 700 Hz.

The numerical simulation allows assessing the acoustic impedance achieved at the interface of the plasmacoustic transducer. Figure 5 shows the real and imaginary part of the impedance calculated as the ratio of average pressure and average normal velocity, the averages being calculated for each transducer over their active area. At low frequencies, the real part of acoustic impedance is exactly  $Z_0$  and the imaginary part is close to 0. As frequency increases, the imaginary part gradually grows but does not exceed 0.15 - 0.2  $Z_0$ . One can also observe the narrowband outbursts of impedance values at both real and imaginary parts. These deviations happen at different frequencies for the four transducers. A more detailed analysis not presented here shows that when the mode shapes become complex at higher frequencies, the pressure node lines can be narrower than the transducer size. This causes the acoustic pressure to be distributed very unevenly over the surface of the transducer. As a result, a single microphone may not estimate well the average pressure over the active surface at a particular frequency at a given location of the transducer. At frequencies above the considered range, the deviations of achieved impedance are expected to grow. A reduction of the transducer's size or a smarter pressure estimation at the interface can mitigate this effect. However, outbursts are not present on all the transducers at the same frequency which helps avoid amplification of sound or other undesired operations that can be confirmed by the noise reduction performance shown in Figure 4.

One of the characteristics of the active sound absorption approach that differentiates it from the noise cancellation techniques is that the noise reduction is observed within the whole space and not only in a relatively small controlled zone. Figure 6 illustrates the global effect in terms of noise reduction. Here, the sound pressure level is calculated as the average value inside a

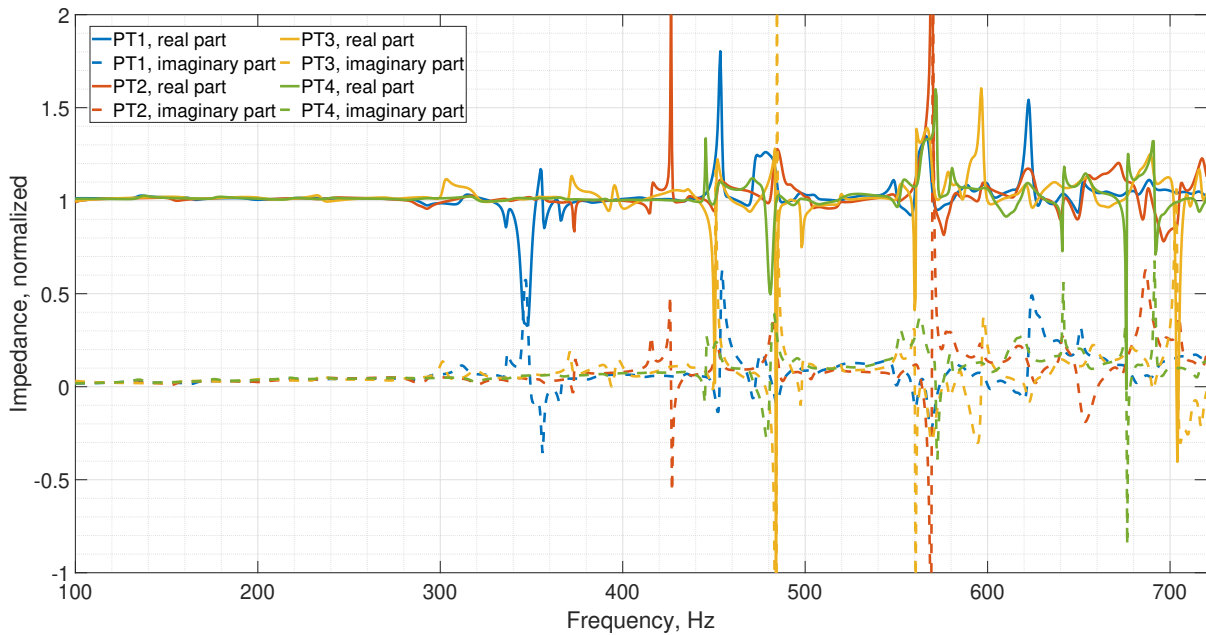


Figure 5: Simulated acoustic impedance achieved across the active surface of four plasmacoustic transducers (PTs in legend). Solid line - real part of impedance, dashed line - imaginary part. Impedance is normalized by  $Z_0$ .

rectangular volume centered with the test volume and smaller by 30 cm in each dimension. Such a representation differs from a measurement at a single point because the low-energy sharp dips of a point response get averaged out. Consequently, the noise reduction effect can be better highlighted. The peaks of the low-frequency modes below 300 Hz are reduced on average by 5 dB or more, and the reduction effect diminishes towards high frequencies. It can also be seen that with the selected positions of the plasmacoustic transducers, some of the high-frequency modes are not tackled by the active control. Increasing the active area can substantially improve the high-frequency performance.

Numerical simulation of the active sound absorption with the plasmacoustic transducers suggests that a broadband and tangible effect on the noise reduction in the test volume can be achieved with a small number of devices. These findings are experimentally verified in the next section.

## 5. EXPERIMENTAL VALIDATION OF PASA SYSTEM PERFORMANCE IN THE TEST VOLUME

The analytical control transfer function used in the numerical simulations is discretized and deployed on a Speedgoat real-time controller. The sampling frequency of the controller is 100 kHz. The microphone senses the acoustic pressure in front of the plasmacoustic transducer prototype and feeds the controller input. The output signal from the controller is amplified with a custom-made high-voltage amplifier and powers the transducer. Each of the four plasmacoustic transducers are driven with an independent SISO control system. The controller targets acoustic impedance  $Z_0$  at the microphone location. The PASA system performance is evaluated with the test volume excited by a broadband noise or a sinusoidal sweep. The recordings are made at various locations in the test volume but for the purpose of comparison with the simulation data, but only the measurement at microphone 1 position (see Figure 1) is presented here. The frequency response with PASA system in passive and active regimes is shown in Figure 7.

The experimental measurements are closely aligned with the simulation data. Although the detailed shape of the passive response and the initial damping of the modes can slightly

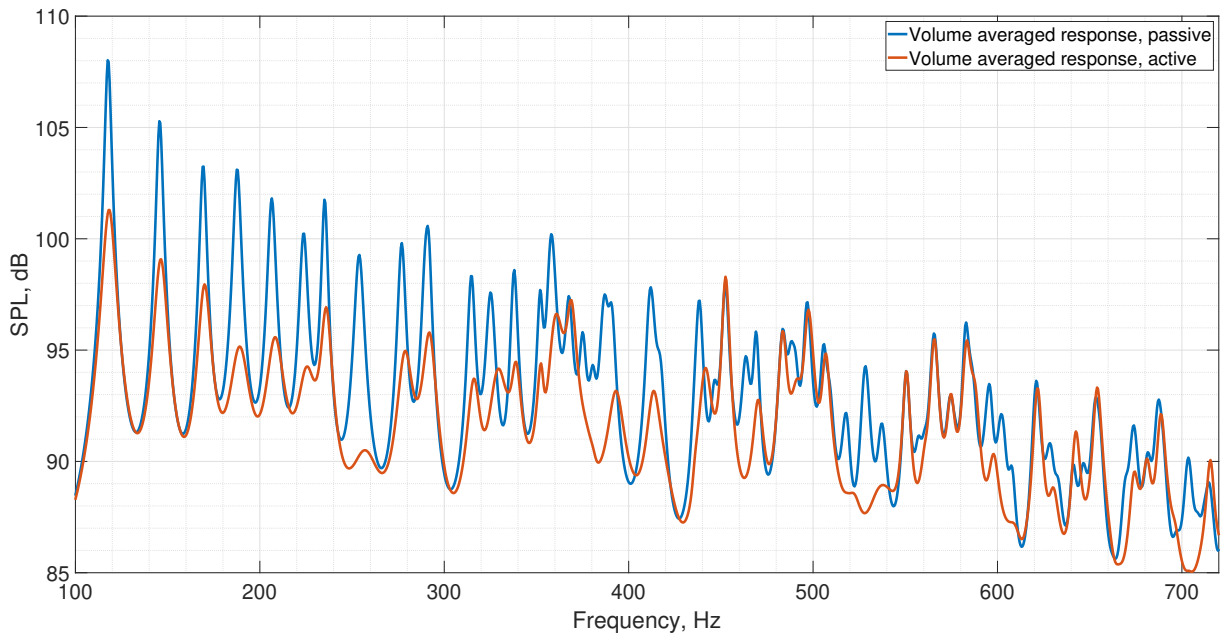


Figure 6: Simulated frequency response averaged over a rectangular space centered with the test volume and smaller by 30 cm in each dimension. Blue - PASA system turned off; red - PASA system targets  $Z_0$  impedance.

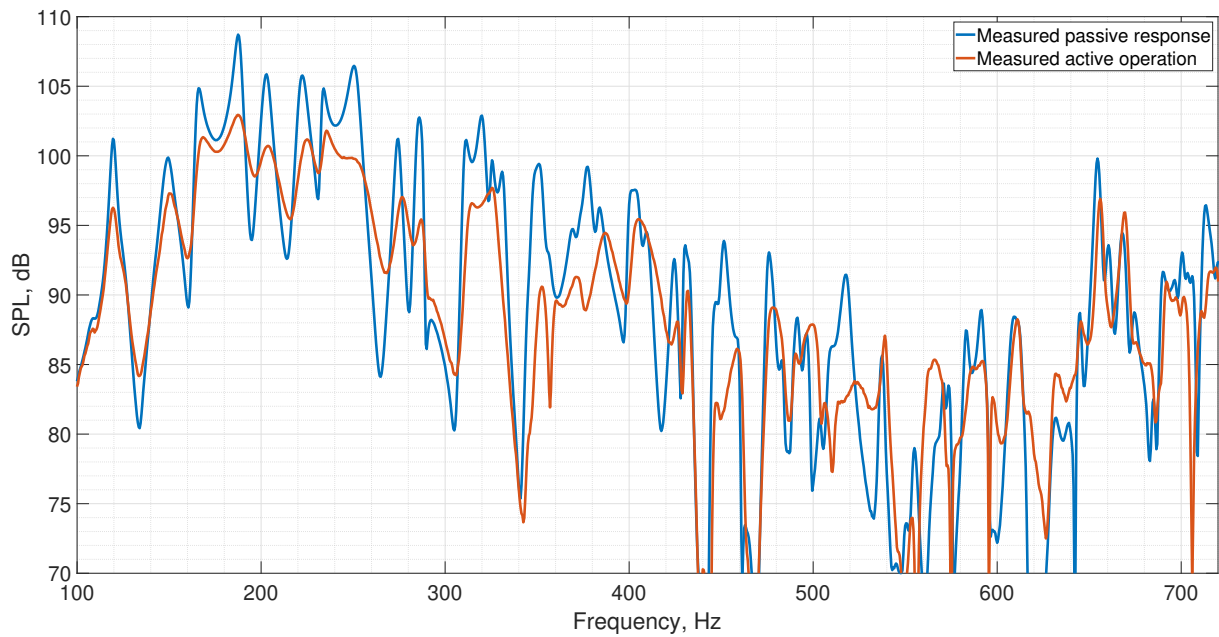


Figure 7: Measured frequency response at a single point of the test volume. Blue - PASA system turned off; red - PASA system targets  $Z_0$  impedance.

differ (discussed in section 2), the relative performance of the plasmacoustic sound absorption system is found to be similar. Low-frequency modes are reduced in magnitude. Some higher frequency modes become indistinguishable, however, some are not considerably changed as was also observed in the simulations. The overall noise reduction calculated over 100-700 Hz was found to be 2.5 dB. It is larger at lower frequencies and slightly smaller at higher frequencies. To augment the noise reduction performance, more active transducers can be added. Alternatively,



a different acoustic impedance can be targeted. Similar sound pressure level reduction and equalization effects were measured at different locations of the test volume. Although the authors do not have means of estimating the achieved acoustic impedance in situ, the verification was performed initially in an impedance tube to ensure that the controlled plasmacoustic transducers are actually set to an impedance close to the targeted one. Moreover, an indirect comparison of measured performance with simulation indicates that the active system operates as intended. Therefore, the experimental validation shows that the PASA system, even with a relatively small number of transducers and active area, is capable of changing the global acoustic behavior of the small three-dimensional volume. Moreover, it allows achieving such a performance over a broad frequency range, which is far more extended than with the active electroacoustic resonators reported in [11].

## 6. TOWARDS THE CONTROL OF A REALISTIC VEHICLE CABIN

In the previous sections, we have concluded that the plasmacoustic active sound absorption system can be efficient in global noise reduction if the space is highly reverberant. However, various spaces present different initial damping. For example, a typical car cabin presents more acoustic losses than the considered test volume due to sound transmission through leakages, vibroacoustic behaviour of the relatively light panels, and absorption by interior materials. Moreover, the total area of active treatment needed to achieve a certain level of noise reduction is proportional to the volume of the space. To evaluate the potential performance of the PASA system in a more realistic case, the numerical simulations are conducted in a generic vehicle cabin model.

Figure 8 presents the geometry of a generic car interior. The geometry was initially taken from COMSOL library model [16] and modified. The goal was to estimate the amount of active sound absorbing surface in order to noticeably ( $\sim 3$  dB) reduce the global sound pressure levels in the cabin, accounting for realistic acoustic environment. Since modeling the acoustic properties of plastic elements, trim materials, and acoustic-structure interaction is a very complex task that may not lead to the correct overall cabin response, and that the purpose here is to check the relevance of the proposed active strategy, a similar approach to the case with the test volume is adopted here. First, the frequency response in several locations was measured in a real vehicle cabin of similar dimensions when excited by a loudspeaker in the trunk. Second, the acoustic boundary conditions of the modelled cabin were adjusted to recreate similar shapes in the simulated and measured SPL responses. Although this is a rather qualitative approach, it can provide a more representative acoustic environment in terms of overall acoustic losses in different frequency ranges.

The following boundary conditions were applied to the cabin surfaces. Windows are treated as boundaries with 3% absorption. The roof and the floor represent a 25 mm thick porous layer with  $20000 \text{ Pa} \cdot \text{s}/\text{m}^2$  flow resistivity coefficient. An absorption coefficient of 15% is assigned to the rest of the surfaces. Such a combination provides relatively high damping from the low frequencies in the model which is represented by structural interaction, transmission and sound leakage losses in the real cabin. High-frequency losses are increased due to the porous layer in the simulation and are represented by a large amount of acoustic absorbing materials in the real cabin.

It was observed in Figure 5 that the impedance achieved by the plasmacoustic transducers closely corresponds to the target value in the considered frequency range. Thus, the potential performance of the PASA system can be evaluated by simply simulating surfaces with assigned acoustic impedance value instead of simulating the whole control loop. This substantially saves computational time since it does not consider the fine mesh for the plasmacoustic metalayer. The numerical study was performed to find the amount of active surface necessary for an overall noise reduction of approximately 3 dB. The example of active surface arrangement is illustrated by the purple areas in Figure 8. At the experimental validation and prototyping stage, the equivalent

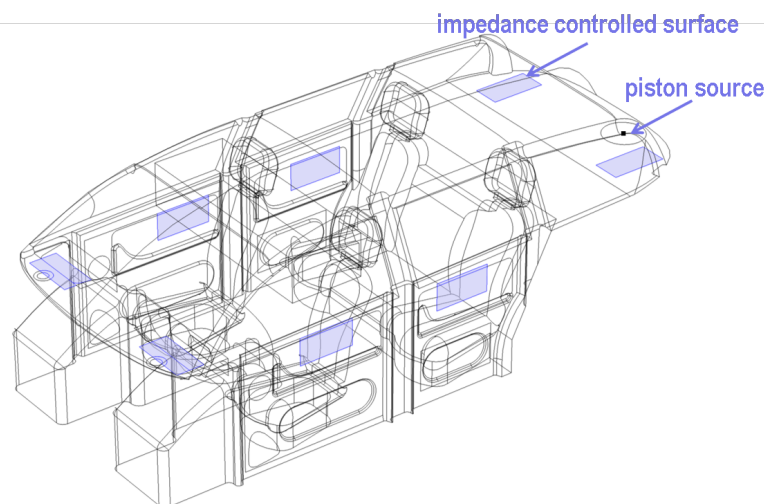


Figure 8: Simulated generic vehicle cabin, total volume  $3.3 \text{ m}^3$ , total area  $23 \text{ m}^2$ . Colored surfaces - acoustic boundary conditions with prescribed acoustic impedance.

amount of active surface can be represented by the required number of plasmacoustic transducers tailored in shape and size to satisfy the design and high-frequency noise reduction performance requirements.

The result of applying constant impedance of  $Z_0$  and  $0.5Z_0$  to the active surfaces is shown in Figure 9. The sound source is a circular piston at the back of the cabin (Figure 8). The response is averaged over a large rectangular volume in front of the driver and front passenger seats (can also be seen in Figure 8). It can be seen that with such high acoustic damping in the simulated cabin, only several first modes can be distinguished. The other modes overlap and result in a rather smooth response due to their low quality factors. The total surface area of treatment equals  $0.4 \text{ m}^2$  which is still very small compared to the total  $23 \text{ m}^2$  of the cabin surface. It was found to be enough to provide 3.7 dB SPL reduction in the frequency range up to 400 Hz and 3.1 dB up to 700 Hz if the assigned impedance equals  $Z_0$ . Targeting lower  $0.5Z_0$  impedance can result in even better noise reduction averaging 5.1 dB up to 400 Hz. Above this frequency, the performance is similar between both active cases. Therefore, even in a highly damped three-dimensional volume, an active sound absorption system set to a broadband impedance control can provide a tangible noise reduction effect that can be observed in the whole cabin space.

## 7. CONCLUSIONS

This work demonstrates the potential of the PASA system to reduce undesired noise in small three-dimensional spaces. The employment of a plasmacoustic metalayer helps substantially extend the bandwidth of a single device to locally control the acoustic impedance. We have seen that four plasmacoustic transducers with  $130 \times 130 \text{ mm}^2$  area (only 0.7% of test volume surface) are enough to reduce noise by 2.5 dB in a highly reverberant empty test volume. In the relatively damped modelled car cabin, the numerical study suggests that  $0.4 \text{ m}^2$  (1.75% of area) of the active area, set to achieve an acoustic impedance  $Z_0$ , should be sufficient to provide more than 3 dB broadband noise reduction. Thus, a realistic environment with substantial initial damping requires larger active areas but can still be controlled with an affordable number of transducers. On the opposite, the same amount of active surface in a lower-damped environment can produce higher noise reduction. It was demonstrated that lower target resistance works better at low frequencies in the simulated car cabin. Although this was already observed in the literature (for example, [11]) finding an optimal target impedance in general is a complex task that requires

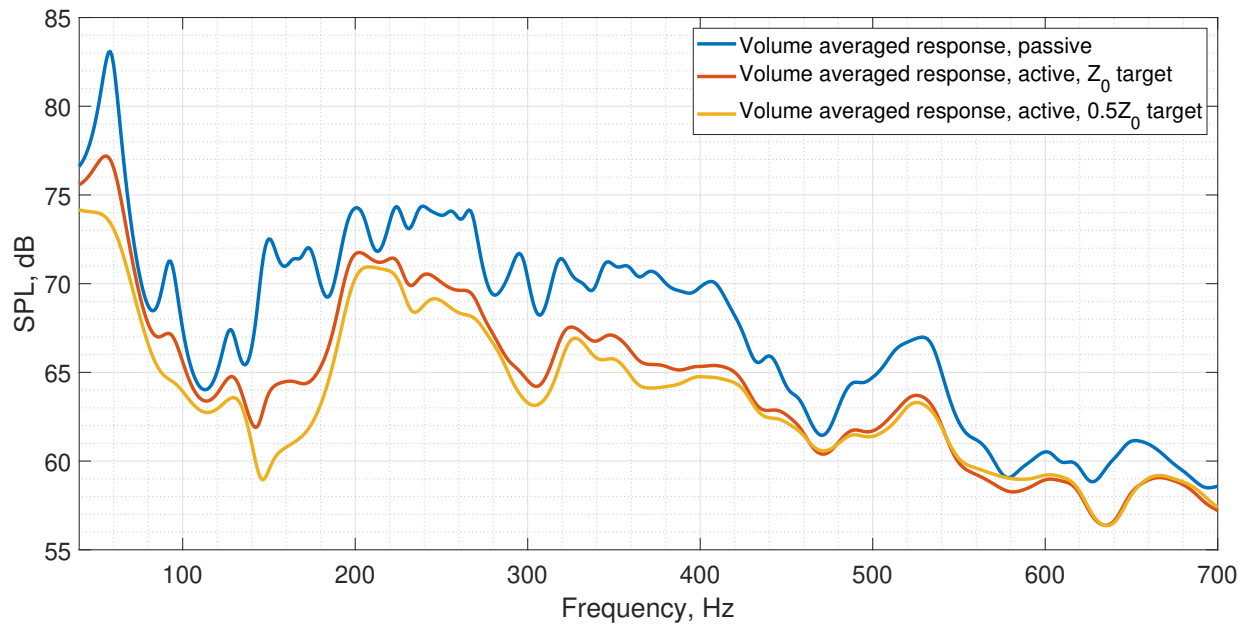


Figure 9: Simulated frequency response averaged over a rectangular in front of the front seats. Blue - passive response; red - active surfaces are assigned  $Z_0$  impedance; yellow - active surfaces are assigned  $0.5Z_0$  impedance.

considering the particular space acoustics, frequency band of control, and constraints on the transducer (e.g., maximum output voltage). To avoid this, a simple-to-implement target such as  $Z_0$  can work relatively well for all scenarios, and the required noise reduction can be adjusted by the number of deployed transducers. To sum up, the active sound absorption system with the plasmacoustic transducers is capable of providing broadband and global noise reduction at a potentially lower cost than an active road noise cancellation system because it does not require numerous accelerometers on the drive train and demands less processing power.

## ACKNOWLEDGEMENTS

The research presented in this document was conducted as part of the PANACHE innovation project, which is supported by Innosuisse, the Swiss Innovation Agency, under grant agreement No. 102.618 IP-ENG.

## REFERENCES

1. Sen M. Kuo, Yi-Rou Chen, Cheng-Yuan Chang, and Chien-Wen Lai. Development and evaluation of light-weight active noise cancellation earphones. *Applied Sciences*, 8(7), 2018.
2. Young-Jae Jang, Jaehyun Park, Won-Cheol Lee, and Hong-June Park. A convolution-neural-network feedforward active-noise-cancellation system on fpga for in-ear headphone. *Applied Sciences*, 12(11), 2022.
3. Juan M Egaña, Javier Díaz, and Jordi Viñolas. Active control of low-frequency broadband air-conditioning duct noise. *Noise Control Engineering Journal*, 51(5):292–299, 2003.
4. Trevor Cox and Peter d’Antonio. *Acoustic absorbers and diffusers: theory, design and application*. CRC press, 2016.
5. SJ Elliott, IM Stothers, PA Nelson, AM McDonald, DC Quinn, and T Saunders. The active control of engine noise inside cars. In *INTER-NOISE and NOISE-CON congress and conference proceedings*, volume 1988, pages 987–990. Institute of Noise Control Engineering, 1988.

6. Shuai Zhang, Lijun Zhang, Dejian Meng, and Xiongfei Pi. Active control of vehicle interior engine noise using a multi-channel delayed adaptive notch algorithm based on fxlms structure. *Mechanical Systems and Signal Processing*, 186:109831, 2023.
7. Trevor J Sutton, Stephen J Elliott, A Malcolm McDonald, and Timothy J Saunders. Active control of road noise inside vehicles. *Noise Control Engineering Journal*, 42(4):137–147, 1994.
8. Shi-Hwan Oh, Hyoun-suk Kim, and Youngjin Park. Active control of road booming noise in automotive interiors. *The Journal of the Acoustical Society of America*, 111(1):180–188, 01 2002.
9. Stephen J Elliott and Jordan Cheer. Modeling local active sound control with remote sensors in spatially random pressure fields. *The Journal of the acoustical Society of america*, 137(4):1936–1946, 2015.
10. Stephen J Elliott, Woomin Jung, and Jordan Cheer. Head tracking extends local active control of broadband sound to higher frequencies. *Scientific reports*, 8(1):5403, 2018.
11. Etienne Thierry Jean-Luc Rivet. Room modal equalisation with electroacoustic absorbers. Technical report, EPFL, 2016.
12. Etienne Rivet, Sami Karkar, Hervé Lissek, Torje Nikolai Thorsen, and Véronique Adam. Experimental assessment of low-frequency electroacoustic absorbers for modal equalization in actual listening rooms. In *Audio Engineering Society Convention 140*, May 2016.
13. Stanislav Sergeev, Romain Fleury, and Hervé Lissek. Ultrabroadband sound control with deep-subwavelength plasmacoustic metalayers. *Nature Communications*, 14(1):2874, 2023.
14. S. Sergeev, H. Lissek, A. Howling, I. Furno, G. Plyushchev, and P. Leyland. Development of a plasma electroacoustic actuator for active noise control applications. *Journal of Physics D: Applied Physics*, 53(49):495202, dec 2020.
15. Stanislav Sergeev, Hervé Lissek, and Maxime Volery. Plasma based noise reduction system, U.S. Patent US11790881B2, 2022.
16. Comsol Multiphysics Application. Car cabin acoustics — frequency-domain analysis. <https://www.comsol.com/model/car-cabin-acoustics-8212-frequency-domain-analysis-15013>.